ARTICLE

Influence of Surface Chemical Modification on Charge Transport Properties in Ultrathin Silicon Membranes

Shelley A. Scott, Weina Peng, Arnold M. Kiefer, Hongquan Jiang, Irena Knezevic, Donald E. Savage, Mark A. Eriksson, and Max G. Lagally*

University of Wisconsin—Madison, Madison, Wisconsin 53706

ABSTRACT Ultrathin silicon-on-insulator, composed of a crystalline sheet of silicon bounded by native oxide and a buried oxide layer, is extremely resistive because of charge trapping at the interfaces between the sheet of silicon and the oxide. After chemical modification of the top surface with hydrofluoric acid (HF), the sheet resistance drops to values below what is expected based on bulk doping alone. We explain this behavior in terms of surface-induced band structure changes combined with the effective isolation from bulk properties created by crystal thinness.

KEYWORDS: silicon-on-insulator · nanomembranes · silicon · electronic transport · surface modification · hydrofluoric acid

In addition to conventional technological drivers for its application,[1,2] silicon-on-insulator (SOI) provides the foundation for a new class of materials, silicon nanomembranes.[3,4] These nanomembranes have unique electronic, mechanical, and thermal properties that have already led to several diverse applications.[5−10] In addition, nanomembranes afford the opportunity to study the extensive influence of surface and interface effects on the electronic properties of Si in the absence of an extended bulk.[11]

Silicon-on-insulator consists of a thick silicon handling wafer, a buried oxide (BOX) and a thin outer Si layer, the template layer, which, either attached or released from the oxide, acts as the nanomembrane. A native oxide forms naturally on the Si template layer. The sensitivity to the surface condition can be illustrated by comparing charge transport in SOI(001) in which the Si(001) template layer is thinned with the outer surface (1) oxidized and (2) cleaned in ultrahigh vacuum (UHV). This experiment, recently performed,[11] shows a sheet resistance that depends strongly on the Si template layer thickness when the surface is oxidized, becoming very high as the Si thickness becomes very small. For conventional doping levels of 10^{15} cm^{-3}, the effect becomes noticeable for membrane thicknesses less than 200 nm, changing 5 orders of magnitude as the thickness is reduced to 10 nm.

When subsequently the surface is cleaned in UHV and shows the 2 × 1 reconstruction (as established by scanning tunneling microscopy (STM)) indicative of the clean surface, the sheet resistance drops significantly, for example, by several orders of magnitude for a 10 nm Si template layer. This low-resistance state was shown to be a consequence of the surface reconstruction, and an interpretation of these data establishes the concept of "surface transfer doping" involving band-like clean-surface states.[11] Similar charge transfer from molecular monolayers into the device channel of a pseudo-MOSFET has also been reported.[12]

The apparent extreme sensitivity of charge transport in very thin SOI(001) to the surface condition, a sensitivity that is absent for bulk Si, suggests the need for a comprehensive approach to understanding potential impacts of structural or chemical modification of the surface on the transport properties. The simplest and most straightforward of these surface modifications would seem to be termination with hydrogen. When the clean surface of thin SOI(001) is dosed with H in UHV, the STM image rapidly degrades and, at coverages of the order of 20% of a monolayer, it becomes impossible to image with STM, an indication that the sheet resistance has rapidly increased. In contrast, bulk Si(001) with H adsorbed is easily imaged.[13] It was

*Address correspondence to lagally@engr.wisc.edu.

Received for review January 30, 2009 and accepted May 25, 2009.

Published online June 5, 2009.
10.1021/nn9000947 CCC: $40.75

© 2009 American Chemical Society

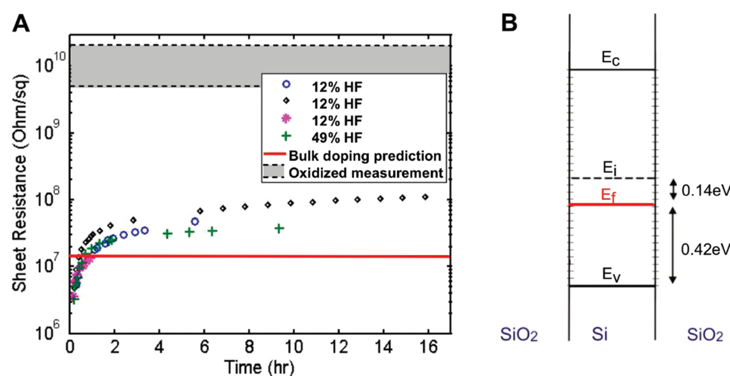

Figure 1. Electrical properties of a 27 nm template layer on SOI(001). (A) Sheet resistance as a function of oxidation time after HF treatment. The first data point is 13 min after HF treatment. The band bounded by the dashed lines represents the range of uncertainty of R_s measured for samples with a native oxide (not measured as a function of time). The solid red line shows R_s calculated for a 27 nm thick Si slab with bulk doping of 10^{15} cm^{-3} only (*i.e.*, no interface states or fixed oxide charges). (B) Band diagram for a 27 nm slab of Si terminated by oxide on both sides, using D_{it} of order 10^{10} cm^{-2} eV^{-1}. E_i represents the intrinsic Fermi level, E_v the valence band, and E_c the conduction band. The band bending at the interfaces is ~0.15 meV and is not visible on the energy scale of the diagram.

suggested[14] that H rapidly destroys the dimer-row-created surface band structure on clean Si that is thought to be necessary for the high conductivity of clean thin Si(001).[11]

Termination with hydrogen is also nominally easily achieved with hydrofluoric acid (HF), and much is already known about the influence of HF treatment on bulk Si surfaces.[15−17] Si(001) surfaces are frequently treated with HF to remove oxide and to provide a H-terminated surface for subsequent device processing. The appeal of this very standard technique lies in the generation of a Si(001) surface that retards oxidation in an ambient environment and provides a low density of surface states.[18−20]

We have explored the conductivity of thin (as thin as 27 nm) p-doped Si template layers of SOI(001) and compared the values if the surface is native-oxide-terminated or HF-treated. A thin nanomembrane of Si conventionally doped at 10^{15} cm^{-3} and terminated on both sides by oxide is effectively intrinsic,[21,22] as articulated below. The same concept applies to Si nanowires, where high doping levels are required to compensate for charge trapping at the Si/SiO_2 interfaces.[23−25] In HF-treated membranes (we use "membrane" and "template layer" interchangeably), the conductance is much higher than is expected if one considers just the number of bulk dopants.[11] In contrast to expectations from H dosing in UHV, our results imply that the HF treatment moves the Fermi level close to the conduction band minimum, resulting in an inversion from the initially nominally p-type to an n-type template layer and a large drop in sheet resistance. We compare our results to observations of surface band bending in HF-treated bulk Si[16,17] and show that, in the ultrathin limit, these near-surface effects completely dominate the electronic properties of the template layer, producing an extreme sensitivity to the local (surface) environment.

RESULTS AND DISCUSSION

Ultrathin Membranes: Sheet Resistance. The sheet resistance of Si squares patterned from ultrathin SOI (UTSOI) was measured in the van der Pauw configuration (see Methods), at room temperature and in a dry environment. Figure 1A shows the sheet resistance as a function of time for four SOI(001) samples with 27 nm thick template layers treated with HF (and a subsequent 5 min distilled, deionized-water rinse), beginning 13 min after HF treatment. For the 27 nm membranes, we measure initial sheet resistances as low as 3×10^6 Ω/sq, with a rapid increase for the first few hours. There is no distinguishable difference in the trend for the samples treated with the standard 12% HF solution and that exposed to 49% HF (discussed later). The band bounded by the dashed lines shows the range of measured sheet resistances of a 27 nm thick Si membrane with a native oxide on the top surface (*i.e.*, the width of the band represents the experimental uncertainty). The solid line shows the calculated sheet resistance of a 27 nm thick Si membrane using only the nominal bulk doping density of 10^{15} cm^{-3} (*i.e.*, no interface states or fixed oxide charge on either side) and assuming an electron mobility of 630 cm^2 V^{-1} s^{-1} and a hole mobility of 250 cm^2 V^{-1} s^{-1}, values appropriate for thin sheets.[14]

The sheet resistance after HF treatment initially increases very rapidly, typically by an order of magnitude in less than 2 h exposure to ambient (dry) atmosphere. The initial phase of oxidation constitutes the formation of a first monolayer of oxide and a continuous reduction in the number of dihydride bonds and has previously been observed to take 2−3 h.[26] The increase in sheet resistance shown in Figure 1 is consistent with the growth of electrically active defects as the initially (primarily) H-terminated Si surface oxidizes.[26,27] After the first 2 h, the sheet resistance increases more slowly and, in the 16 h plotted in Figure 1, remains almost 2 orders of magnitude lower than measured for a fully oxidized sample. After several weeks, the sheet resistance finally approaches the value for the native-oxide-terminated surface.

It is clear from Figure 1A that the initial value of sheet resistance after the HF treatment is several orders of magnitude lower than that of an oxidized SOI sample with the same thickness and is also lower than that expected for the ideal case of a Si slab considering only the bulk dopant concentration. The number of dopants in the template layer of a 27 nm thick SOI sample (nominal manufacturer doping ~10^{15} cm^{-3}) is around 3×10^9 cm^{-2}. The number of free carriers is determined by interface charge trapping at the back Si−SiO_2 interface.[28] Typical values of interface trap density (D_{it}) range between 10^{10} and 10^{12} cm^{-2} eV^{-1}.[21,22,29]

Even in the lower limit of $D_{it} \sim 10^{10}$ cm^{-2} eV^{-1}, the interface trap density in the gap is greater than the number of dopants in the 27 nm membrane, rendering the membrane effectively intrinsic, with a Fermi level ~0.14 eV below mid gap,[14] as shown in Figure 1B, rather than 0.3 eV below mid gap, as would be the case for a bulk Si sample with the same p-type doping concentration. Consequently, the membrane should be extremely resistive if the front surface is simply well-passivated (within a factor of 2 of the sheet resistance measured for the oxidized sample because the buried oxide (BOX) remains) and if no additional interface states or surface charges are introduced by the HF treatment. Comparison of the initial sheet resistance after HF treatment with the calculated value of sheet resistance assuming only bulk doping (10^{15} cm^{-3}) with *no interface states on either side of the membrane* reveals that the values for the HF-treated 27 nm membranes are almost an order of magnitude lower than if there were no traps at all (bulk doping only).

The bulk-doping-only calculated value serves only as a point of reference for the measured values of sheet resistance. In reality, there may be fixed oxide charge in both the top native oxide and the bottom BOX.[30,31] The observation that HF treatment reduces the sheet resistance by several orders of magnitude compared to that measured for the oxidized sample cannot, as we will explain, be attributed to removal of fixed charge with removal of the top oxide layer nor, we believe, by the possible remaining presence of a fixed charge in the BOX.

Ultrathin Membranes: Carrier Concentration and Type. Carrier concentrations and type were determined from Hall effect measurements (in the van der Pauw geometry) in a physical-property measurement system (PPMS), under a rough vacuum of a few Torr. Pumping the system serves two purposes. First, the oxidation rate of the surface is significantly reduced, allowing measurement of a large data set with only minor changes in the surface condition. Second, pumping removes ambient water to allow comparison with the sheet resistance measurements that were taken in a dry atmosphere. We also performed several van der Pauw measurements in the PPMS system at zero magnetic field after pumping to correlate directly the sheet resistance with the carrier concentrations at the same stage of oxidation.

The Hall resistance ($R_H = V_H/I$) is plotted as a function of applied magnetic field in Figure 2A for a 27 nm thick membrane, 23 min after HF treatment. The sign convention is schematically depicted in Figure 2B. A sheet resistance measurement after pumping yields a value of $R_s = 3.4 \times 10^7$ Ω/sq, consistent with measurements in the dry purged environment. In Figure 2A, it is immediately obvious from the negative slope that the

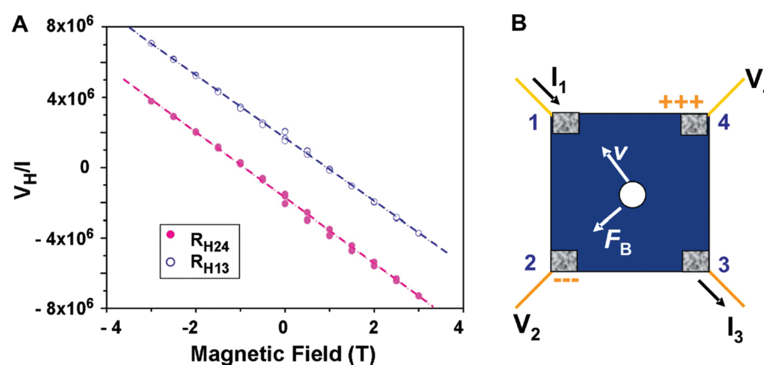

Figure 2. Hall effect measurements on 27 nm SOI(001). (A) Magnetic field dependence of the Hall resistance. The two plots correspond to current passed between contacts 1 and 3 with voltage measured across contacts 2 and 4 (R_{H24}) and current passed between contacts 4 and 2, with voltage measured across contacts 1 and 3 (R_{H13}). The offset from zero of both the lines (in opposite directions) likely results from errors in symmetrically positioning the probe contacts. (B) Schematic diagram of the contact geometry and sign convention (positive magnetic field points out of the page) with electrons as the charge carriers.

membrane features n-type conduction and hence an inversion from nominal p-type SOI to n-type. The Hall resistance is related to the carrier density, n, through the expression

$$n = \frac{B}{edR_H} \quad (1)$$

where d is the membrane thickness, B is the magnetic field, and e is the electronic charge,[29] yielding a carrier concentration of $n = 1.3 \times 10^{14}$ cm^{-3}.

Discussion in Light of Past Observations. The conductivity as a function of oxidation time of relatively thick (1 μm) HF-treated SOI(111) with nominal n-type doping has recently been investigated.[27] A similar increase in the sheet resistance with oxidation is observed for this different orientation of Si, as the H termination is replaced with a native oxide and consequently a higher density of interface traps. Note, however, that ref 27 finds an initial resistance after HF treatment comparable to that expected for the sample's bulk doping level (*i.e.*, a well-passivated surface, no effect of interface states trapping charge). Our membranes are thin enough that the interface trap density in the gap exceeds the sheet density of dopants, and hence, the dopant charges are depleted by traps at the Si/BOX interface, as we have stated (*i.e.*, the Fermi level is close to midgap). When the native oxide is removed, these back interface traps remain and continue to be active. They should therefore cause the initial resistance after HF treatment to be *higher* than what one would observe for a bulk sample with the same nominal doping density. In contrast, our membranes, as shown in Figure 1A, have an initial sheet resistance that is *significantly lower* than predicted even for bulk doping in the complete absence of interface traps.

There have been several reports of band bending in the near-surface region of bulk Si after HF treatment, using X-ray photoelectron spectroscopy (XPS)

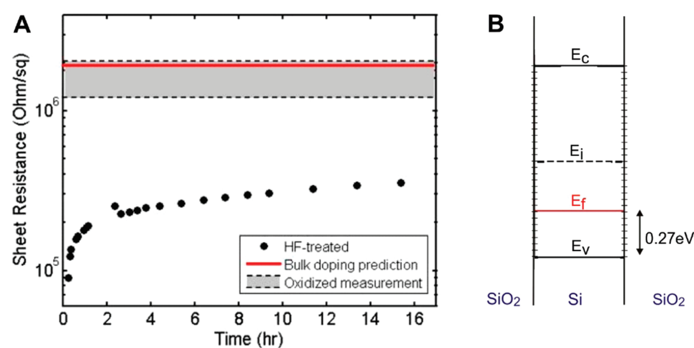

Figure 3. Electrical properties of 220 nm SOI(001). (A) Plot of the sheet resistance as a function of oxidation time after HF treatment. The first data point occurs 25 min after the HF treatment. The band bounded by the dashed lines represents the range of uncertainty of measured sheet resistances for samples with a native oxide (not measured as a function of time). The solid red line, the predicted sheet resistance for a perfectly passivated surface (*i.e.*, no surface states on either side of the template layer), lies within this band, as expected for membranes this thick or thicker. (B) Simple band diagram for oxidized 220 nm thick, nominally p-doped SOI(001), calculated using $D_{it} \sim 10^{10}$ cm^{-2} eV^{-1},[14] $E_c - E_v = 1.12$ eV. The Fermi level is located at 0.27 eV above the valence band, consistent with the Fermi level position of a bulk Si sample with equivalent doping.

and surface photovoltage (SPV) methods.[15−17] For both (001) and (111) orientations, they generally show the surface Fermi level positioned near the bottom of the conduction band, even for p-doped Si, with no obvious orientation dependence. (One study observed a reduction in band bending with oxidation time.[16]) This band bending has little effect on the overall electrical properties of the bulk material (hence, sheet resistance measurements are not useful for bulk Si), as the width of the depletion region (although dependent on doping and the surface potential) typically extends only of order 1 μm into the Si bulk. In contrast, the template layer in our ultrathin SOI(001) is much thinner than the typical depletion width. If we estimate the Fermi level position ($E_c - E_F$) using the expression

$$n = N_c e^{-(E_c - E_F)/kT} \quad (2)$$

where N_c is the effective density of states in the conduction band,[29] for our 27 nm layers (using $n = 1.3 \times 10^{14}$ cm^{-3}, extracted from our Hall measurements), the Fermi level is positioned at 0.32 ± 0.03 eV below the conduction band minimum for data averaged across three identically prepared samples. This value is consistent with the observations, by other methods, of the position of the Fermi level at the surface of bulk Si(001) treated with HF.[15−17]

Schlaf *et al.*[17] have shown that the Fermi level at the surface of bulk Si is pinned within ~0.2 eV of the conduction band for a wide range of doping. For our thin membranes, the details of the profile of the bands with depth into the membrane are determined by the interplay of the back Si/SiO_2 interface, the thin "bulk", and the HF-treated surface. As any surface state density that may be introduced by the HF treatment likely exceeds that of the Si/SiO_2 interface trap density,[17] a near flat-band condition when using eq 2 is a good approximation.

Thicker Nanomembranes: Carrier Type and Concentration. The observations on bulk Si(001)[15−17] and our measurements on 27 nm UTSOI(001) indicate that the carriers are electrons after HF treatment, and that the electron concentration decreases with oxidation. Oxidation eventually reverts the membrane to near-intrinsic. We expect that the p-type conductivity should be recovered after oxidation, but we were not able to check this for the 27 nm membranes because the increasingly high resistivity soon made the experiment impossible. Consequently, we measured 220 nm thick membranes, for which the sheet resistance is much lower, prepared in the same manner. Figure 3A shows the sheet resistance as a function of oxidation time for a 220 nm membrane with nominal (10^{15} cm^{-3}) p doping. Similarly to the 27 nm membranes, the initial sheet resistance is much lower than can be accounted for by bulk doping alone, with a rapid increase in sheet resistance with oxidation. The band bounded by dashed lines indicates the measured range of sheet resistance for 220 nm template layers with a native oxide. The solid (red) line is the calculated value of sheet resistance after eliminating all interface traps (*i.e.*, bulk doping only) and again assuming the reduced mobility values. The agreement of the measured and calculated values (within experimental uncertainty) demonstrates that charge transport properties in the thicker membrane are negligibly affected by interface trapping (*i.e.*, the presence of the BOX),[14] further confirming that the initially low sheet resistance upon HF treatment is not simply a consequence of removal of native oxide interface traps. Figure 3B shows a simple band diagram for a 220 nm oxidized Si membrane, where the Fermi level is calculated to reside 0.27 eV above the valence band maximum, the same position as a bulk sample with equivalent doping.

The corresponding carrier density and sign were determined from Hall effect measurements. Figure 4 shows the Hall resistance as a function of magnetic field for the 220 nm sample after 25 min of post-HF-treatment oxidation and after 27 days oxidation in an ambient environment. It is clear from the negative slope at both stages of oxidation that electrons are the carriers. Twenty-five minutes after HF treatment, $n = 1.9 \times 10^{15}$ cm^{-3} ($R_s = 1.7 \times 10^5$ Ω/sq under pumping, consistent with measurements in the drybox). After almost 4 weeks of oxidation, the carrier density drops to $n = 1.7 \times 10^{14}$ cm^{-3} with an increase in sheet resistance to $R_s = 1.7 \times 10^6$ Ω/sq. The increase in sheet resistance and reduction in carrier concentration are consistent with destruction of the hydrogen termination by oxidation, and the observation of electrons rather than holes as charge carriers *initially* is consistent with prior work.[15−17] However, the observation that electrons *continue* as charge carriers is not consistent with the expectation

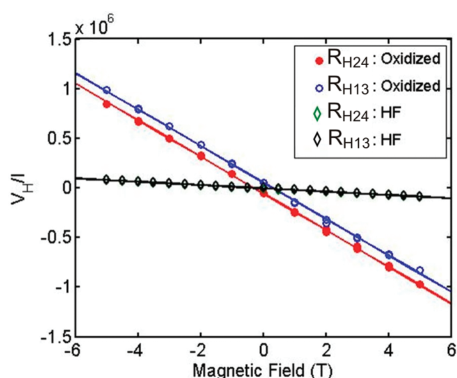

Figure 4. Hall resistance (V_H/I) as a function of magnetic field for 220 nm conventionally (10^{15} cm^{-3}) p-doped SOI(001) samples, immediately after (within 25 min) treatment with HF (indicated by the legend, the two sets of data points coincide), and following 27 days of oxidation. The negative slope indicates electrons are the majority carrier. The steeper slope of the oxidized sample indicates a reduction in carrier concentration.

of a simple reversion back to the bulk p-type template layer after reoxidation.

For situations where the depletion width is expected to be much less than the Si thickness, for example, for bulk Si (or very thick, bulk-like SOI) or highly doped SOI, we would expect HF treatment to exert negligible influence on the electronic properties, as the bulk now dominates the system. In these situations, a p-type sample should remain p-type after HF treatment. We performed Hall measurements on a highly doped (expected doping of order 10^{19} cm^{-3}, corresponding to a Debye length, $L_D \sim 1$ nm) p-type 220 nm HF-treated sample to confirm this expectation.

Figure 5 shows the Hall measurements for the highly doped 220 nm sample. Data points include measurements taken while pumping (vacuum of 1 Torr) and in ambient conditions with the relative humidity (RH) = 22% (indicated by the legend), with no distinguishable difference between the two. The positive slope confirms the p-type carriers, and we extract a carrier concentration of $p = 1.0 \times 10^{19}$ cm^{-3}, consistent with the expected dopant density for our B spin-on dopant recipe. Note that the role of ambient water is also insignificant, with the data points for the ambient system coinciding with those under pumping. As will be shown later, water plays a large role in the electrical properties of SOI, but in the highly doped sample, this is not the case, as the surface plays less of a role in the properties of the system as a whole. Figure 5 confirms that the surface treatment now has negligible effect on charge carrier transport. For this high doping level, surface band bending is localized near the surface, with the unmodified bulk bands occupying the vast majority of membrane thickness. We also measured the carrier type on a 2300 nm thick nominally p-type template layer of SOI(001) (from a different wafer) and again observed a Hall voltage consistent with a p-type sample. We, therefore, conclude that the strong influence of the HF treatment on the electrical properties of very thin SOI is a consequence of the sample thinness and the low doping level. These factors allow surface-induced band modifications to extend throughout the thickness of the nanomembrane, thereby dominating the system behavior. Similar band modifications dominating a thin system can be observed in Si nanowires, where instead of a surface modification a gate bias applied to a wire with low p doping results in inversion to n-type conduction.[32]

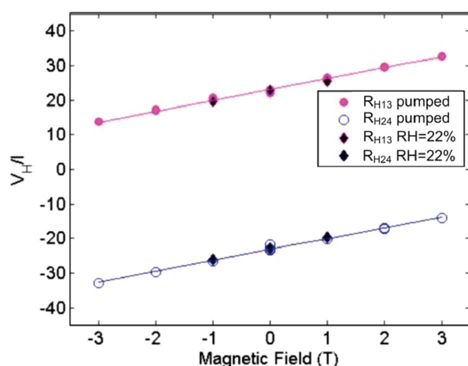

Figure 5. Hall resistance (V_H/I) as a function of magnetic field for a highly doped 220 nm SOI(001) sample immediately after treatment with HF. Measurements were taken in both an ambient and a pumped environment (indicated by the legend, where RH refers to the relative humidity of the ambient samples). The positive slope indicates the carriers are holes. The offset relative to zero is again likely due to contact geometry.

HF at the Si Surface: Discussion and Prior Results. As already alluded to earlier, the influence of HF on the near-surface band structure of bulk Si has been investigated over several decades, but often with contradictory findings. Earlier work found negligible shift or pinning of the near-surface Fermi level after HF treatment,[33,34] while more recent studies find that the Fermi level is indeed shifted[16,17,26,35] and even pinned near the conduction band minimum for a wide range doping levels.[17] However, to date, there is no definitive agreement on the cause of the Fermi level shift, with suggestions of positive surface charge[26] and donor-like surface states[17] existing in the literature, with both attributed to residual species other than hydrogen in the HF etch process.

Band bending in Si with a purely H-terminated (*i.e.*, in the absence of any other chemical species) surface is generally thought to be very small because of passivation of the surface dangling bonds.[36] Our own preliminary work on UHV H-dosing of UTSOI also suggests that pure hydrogen does not increase the conductivity, rather it reduces the conductivity of UHV-cleaned samples by destroying the surface states that arise from the clean reconstructed surface.[11]

Using XPS and SPV, Schlaf *et al.*[17] find a large shift in the near-surface Fermi level after HF treating bulk Si, both n-type and p-type, and (001) and (111) orientations and attribute the band bending to fluorine provid-

ing donor-like surface states. They determined that all sample surfaces contain traces of F and that more dilute etch solutions tend to produce lower surface concentrations of F, in agreement with earlier studies.[18,37] They did not, however, observe any marked change in the surface Fermi level position with varying concentrations of HF, implying a saturation effect of F at low F coverage. They propose that only 0.1% of surface atoms need to be involved in the pinning process (if F is indeed influencing the surface Fermi level position). Watanabe *et al.*[16] used SPV combined with the Kelvin method to probe the surface band bending, and on the basis of Schlaf's findings, they also suggest band bending in bulk Si(001) arises from residual F present on the surface (they observe 0.3% F coverage for 4.5% HF after 10 min rinse).

An upward shift of the near-surface Fermi level position of p-type bulk Si(001) (although less than in the other reports[16,17]), after HF treatment, has also been shown by Huang *et al.* *via* XPS.[19,35] In contrast to Schlaf *et al.*,[17] the Fermi level shift was shown to depend on the HF concentration. They attributed the shift to boron dopant deactivation *via* hydrogen incorporation and the formation of an H−B−Si complex or H−B pairs. They propose that the observed shift with increasing HF concentration is a result of the increased concentration of hydrogen in the aqueous solution. There is a discrepancy here[19] with later work, in that only HF concentrations greater than 10% produced any band bending at all, and the degree of band bending even in 50% HF solutions is much less (E_F still resides well below mid gap) than others have observed. Independent of that, B-dopant deactivation could play only a minor role for our thin membranes, as they are effectively already depleted of charge carriers *via* the interface states. In any case, this proposed mechanism would produce an effect opposite to what we observe, that is, an increase in sheet resistance and no inversion upon HF etching.

Angermann *et al.* observe a strong dependence of the surface Fermi level position in bulk Si [both (001) and (111)] on HF concentration;[15] however, their interpretation of the mechanism is different from that of Schlaf *et al.*[17] Rather than donor-like surface states, Angermann *et al.* suggest that the band bending results from a positive surface charge induced by electronegative surface groups such as OH bonded to the surface Si atoms (note there is only a small electronegativity difference between Si and H, so Si−H bonds, although most prevalent, would only contribute marginally), which would produce an effect similar to a permanent positive gate voltage. Reducing the HF concentration was found to reduce the positive surface charge. From Figure 1, it is apparent that we do not observe any distinguishable dependence of the sheet resistance on the HF concentration.

While the studies discussed above all show a shift in Fermi level toward the conduction band minima after HF treatment, several earlier investigations in the literature do not observe any band bending.[33,34] Our results are in agreement with the more recent studies.[15,17]

There have been extensive studies on the surface species present after treating clean bulk Si with HF.[18,37,38] For Si(001), high-resolution electron energy loss spectroscopy (HREELS) shows a predominance of Si dihydride[38] [in contrast to Si(111), which is dominated by Si monohydride]. Residual species of F and OH groups are also detected, and their concentration exhibits a marked dependence on both the HF concentration and the rinse time after the HF dip. The F and OH coverages are reduced and increased, respectively, in more dilute solutions. Rinsing the samples in water after the HF treatment lowers the F coverage *via* the substitution reaction $Si{-}F + H_2O \rightarrow Si{-}OH + HF$, consequently resulting in an increased presence of OH groups. Our own XPS survey shows no difference (as expected) from the bulk results, namely, no significant oxidation in the time scale of our first sheet resistance measurement after HF treatment and residual surface species consistent with the bulk XPS measurements. The F concentration for our preparation is estimated to be between 0.3 and 1% of a monolayer based on bulk studies.[16,17] Regardless of the precise mechanism (either surface charge or donor-like surface states which is not determinable from our current data), the HF surface treatment completely dominates the electrical properties of UTSOI(001). On the basis of prior results for different orientations of bulk Si,[15−17] we expect the dominance of the surface treatment we see here to occur as well for other orientations of UTSOI.

The sensitivity to the surface is further emphasized by the effect of water. A large jump in resistance is observed when the system is pumped/purged to remove ambient water. Dubey *et al.*[27] correlate the water dependence of the conductivity of the template layer of SOI(111) with Hall measurements and suggest that adsorbed water causes an accumulation of majority carriers for their n-type samples. Our preliminary measurements were performed in an ambient atmosphere, and we observed, in agreement with ref 27, that ambient water produces a dramatic reduction in sheet resistance. Indeed, the effect is so strong that it is difficult to obtain reproducible data due to fluctuations in the lab humidity of up to 10% in less than 1 h. To give an indication of the variation with humidity, $R_s = 2.5 \times 10^6$ Ω/sq after 25 min oxidation in an ambient environment with RH = 51%, while an identical sample in a dry environment (RH $< 5\%$) yielded $R_s = 8.5 \times 10^6$ Ω/sq after the same exposure time to the ambient. A change in sheet conductance of this magnitude ($\sim 3 \times 10^{-7}$ S) can not be accounted for by surface conduction through the adsorbed water layer alone, as previous reports of surface conductance on Teflon and quartz surfaces at typical values of ambient humidity are $<10^{-16}$ S.[39]

It is therefore necessary to reduce and monitor the humidity during measurements to isolate the opposing effects of humidity (reduces R_s) and oxidation (increases R_s) on the sheet resistance. For this reason, the sheet resistance was measured after the drybox reached its stable base humidity of $<$5%. It is unlikely that the substitutional reaction described above could contribute to the dependence of sheet resistance on humidity, as the appearance of surface OH groups is followed by a rupture of Si−Si bonds and formation of Si−O−Si bridges in the lattice.[18] Clearly this is not an easily reversible reaction, as is required for the sheet resistance to decrease after the humidity drops. Rather it is more likely a physisorption effect, where the molecules can be displaced from the surface.[27]

Summary of Results and Discussions. We briefly summarize our findings here and state what we can and cannot conclude on the basis of our findings. (1) Conventionally doped SOI with template layers thinner than 220 nm and a native oxide shows increasingly high sheet resistance as the template layer gets thinner, and in any case higher than one would expect from bulk doping alone. (2) We see a very large reduction in sheet resistance when we expose the top surface of SOI to HF. The sheet resistance slowly (over weeks) increases as the surface reoxidizes. These results hold for membranes at least up to 220 nm at p doping levels of 10^{15} cm^{-3}. For thicker template layers, or much higher doping concentrations, bulk behavior is observed. (3) For nominally p-doped thin membranes (at least less than 220 nm, doping level 10^{15} cm^{-3}), the carrier changes to n-type upon exposure of the surface to HF and appears to remain n-type after native oxide formation. (4) The initial sheet resistance upon exposure to HF is sensitive to adsorbed water.

The observation of a large drop in sheet resistance, accompanied by an inversion to n-type conduction for UTSOI after HF treatment, is consistent with previously reported band bending in the near-surface region of bulk Si after treating with HF. However, for UTSOI, this surface modification dominates the transport properties of the system, as further evidenced by the influence of adsorbed water on the conductivity.

For the thicker (220 nm) oxidized samples, the observation that inversion continues (although the carrier density is reduced, consistent with the drop in sheet resistance) even after reoxidation is likely caused by fixed charge in the regrowing native oxide. Fixed oxide charge is generally positive and resides very close to the Si/SiO_2 interface. It is known to exist in both the native oxide and the buried oxide layer of SOI(001)[30,40,41] but may be higher in the native oxide. Fixed oxide charge can provide an effect similar to a positive gate bias. One can conjecture that as the species responsible for shifting the Fermi level near the conduction band minimum are replaced by O on the surface the fixed oxide charge builds up at the surface and acts as a gate to maintain a weak inversion.

However, the removal of a fixed oxide charge (in addition to the removal of the top interface traps) *via* native oxide stripping in HF cannot account for the drop in sheet resistance we observe. Positive fixed oxide charge may serve to deplete the membrane. Removal of this positive charge would lead to less depletion, which would result in a lower sheet resistance, but in this case, the carriers would be holes rather than electrons as we have shown. If there is enough fixed oxide charge to produce inversion, stripping the native oxide would produce less inversion, leading to an *increase* in sheet resistance, that is, the opposite of our observations. If, on the other hand, we were to assume any inversion was caused by fixed oxide charge in the BOX, and that simply stripping off the top interface traps allows more inversion charge in the membrane, then thin membranes imaged under UHV by STM should not need the surface bands induced by the 2×1 reconstruction to enable conduction. We have shown previously that this is not the case,[11] and as we have mentioned, dosing with atomic H, which is thought to disrupt the clean surface bands, results in a loss of conduction.[14] Clearly the HF treatment either increases the positive surface charge or introduces donor-like surface states, most likely *via* residual species (*i.e.*, other than hydrogen) present on the surface after the HF treatment. Both of these scenarios have been suggested in the literature for HF-treated bulk Si surfaces, as we have discussed.

CONCLUSIONS

The electronic transport properties of ultrathin SOI(001) are extremely sensitive to the surface condition. We have shown that 27 nm SOI(001) treated with HF has a sheet resistance orders of magnitude lower than can be accounted for by a good surface passivation. Hall measurements reveal that the HF treatment produces an inversion from a nominally p-type to an n-type template layer, with the Fermi level estimated to reside at 0.32 ± 0.03 eV below the conduction band minimum, consistent with prior XPS and SPV studies on bulk Si. Unlike bulk Si, however, where surface effects have little influence on the electronic transport properties, UTSOI offers the opportunity to isolate the surface from the extended bulk, with the consequence that surface effects induce a significant modification of the position of the Fermi level throughout the system and completely dominate the electronic transport properties.

The extreme sensitivity of electronic properties to the surface environment that we have demonstrated by the simple example of HF treatment suggests caution in interpretation of transport measurements for devices based on ultrathin SOI and may impact the choice of processing method for SOI for such devices[12,42] and indeed for Si nanowires (SiNWs).[43]

ARTICLE

SiNWs have attracted a great deal of attention for chemical and biosensing because, like UTSOI, their large surface-to-volume ratio makes them very sensitive to their local environment. For small-radius SiNWs with low doping and a native oxide, the wires are fully depleted of mobile charge,[44] rendering them highly resistive, but it is possible to use gating to induce a conducting channel.[32] Conversely, highly doped wires can be used to maintain conduction in the presence of an oxide layer, without the use of gating. In this architecture (nanoscale cross section), the SiNW is driven into either accumulation or depletion when a target species binds to the surface (oxide, functionalized with selective receptor molecules), producing a small conductance modulation in the wire in a manner similar to an applied gate voltage.[25,45,46] For sensing devices formed from SOI, back gating (pseudo-MOSFET geometry) is generally used to form the conduction channel and increase the sensitivity of the device. Subsequent changes, for example, in ion concentrations or surface charge, at the top oxide surface are detected *via* a modulation in current, akin to applying an additional gate voltage.[47,48]

Our observations suggest considerable promise for alternate approaches to biological or chemical sensing. Without the oxide to trap charge, the conductivity change in a uniform sheet of UTSOI is very significant with small changes in surface condition. In addition, functionalization of the clean Si surface can produce excellent binding specificity and longer-term stability than on SiO_2 surfaces.[49,50] If appropriate surface specificities can be adopted from prior work on bulk Si or other group IV materials, attachment of chemically or biologically selective receptor molecules to this clean surface may allow very sensitive molecule-specific sensing using simply the monitoring of sheet resistance across a slab or ribbon of UTSOI.

METHODS

Sample Preparation. Ultrathin SOI (UTSOI) samples with a Si(001) template layer thickness of 27 nm (measured by X-ray diffraction) were prepared by cycles of thermal oxidation and buffered oxide etching (BOE) from commercially available (Soitec) 220 nm p-type (10^{15} cm^{-3} B-doped) SOI wafers. A buried oxide layer thickness of 3 μm was chosen to avoid potential current leakage from the template layer to the bulk handle wafer. Highly doped (B) samples (for comparison to the standard nominal doping) were obtained by spin-on doping (B-150, Honeywell), followed by dopant diffusion and activation with a rapid thermal anneal at 800 °C in a nitrogen environment. This recipe is known to yield an averaged dopant concentration of order $\sim 10^{19}$ cm^{-3}.

Si squares (4 mm × 4 mm) were patterned from the template layer as depicted in Figure 6. Unless otherwise noted, the H-terminated surface was prepared by native oxide stripping in dilute HF, piranha solution (H_2SO_4/H_2O_2) for 10 min, 12% HF for 1 min, 5 min rinse in 18.2 MΩ distilled deionized (DI) water, and a nitrogen blow dry. For electrical measurements on such thin layers, it is important to maintain a smooth and uniform surface after processing. This procedure of thermal oxidation/stripping, chemical cleaning, and H termination produces a thickness variation of <1 nm over the length scale of the samples and an rms roughness of 0.25 nm averaged over several samples, as determined by atomic force microscopy (AFM). A representative AFM scan is shown in Figure 6B. XPS measurements produced spectra consistent with those observed for HF etching of bulk Si(001);[34,38] that is, a surface that shows O, C, and trace F contamination. High-resolution scans of the Si peak showed no chemically shifted peak corresponding to oxide formation for the freshly etched samples. X-ray absorption spectroscopy measurements of the *onset* of photoemission (2p to vacuum level, *i.e.*, the photoelectric effect) show evidence of oxide formation only after several hours.[51]

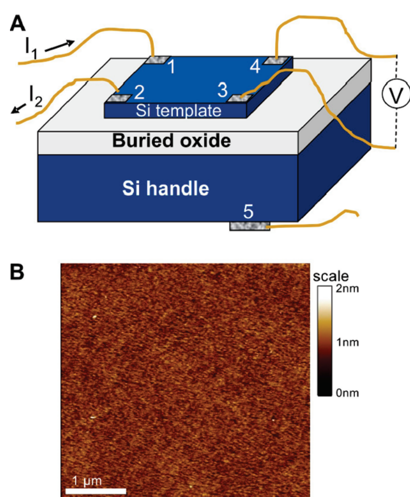

Figure 6. Sample preparation for van der Pauw measurements. (A) Schematic diagram of the sample geometry: an electrically isolated square of Si is contacted with In dots after HF treatment. The current is passed between contacts 1 and 2, and the voltage is measured across contacts 3 and 4. (B) AFM scan of the surface after thinning, cleaning, and HF treatment.

van der Pauw Measurements. Immediately after sample drying, In contacts are soldered under a microscope to the four corners of the Si mesa, and each corner is connected to a high-input-impedance (10^{16} Ω) source measurement unit (Agilent 4156 C). The sheet resistance of each sample is measured *via* the van der Pauw technique,[52] and unless otherwise stated, all measurements are performed in the dark in a dry environment (dry air, <10 ppm water, flowed through a control box with relative humidity <5%). A source current (I_1) is applied to probe 1 and the output current (I_2) measured and compared to I_1 at probe 2. The voltage is measured between probes 3 and 4, as indicated in Figure 6A. The source current is adjusted so that the voltage between probes 3 and 4 is large enough to reduce noise (>1 mV) but low enough to avoid carrier injection (<100 mV). The current is typically swept across the range ±5 nA. We ensure that ohmic-like contacts are obtained, in which case we observe that V_{34} has a linear and symmetric dependence on I_1, which is not the case in occasional instances when we obtain unstable or Schottky-like contacts (these samples are discarded). Four permutations of current/voltage configuration are measured. A fifth probe was connected to either the side wall or the back side of the handle wafer and the current measured between probe 1 and probe 5. Occasionally a current (leakage) was recorded at probe 5, indicating a conducting pathway between the template layer and handle substrate. In these instances, $I_1 \neq I_2$ (some of the source current is lost to the handle wafer). Samples with $I_2 < 0.99\, I_1$ (*i.e.*, greater than 1% leakage current) were discarded. During measurements, the fifth contact was used to ground the

Si handle, and I_2 monitored to provide real time identification of current leakage.

Hall Effect Measurements. Hall measurements were performed in a physical-property measurement system (PPMS) (Quantum Design) at a rough vacuum of a few Torr, using the van der Pauw geometry depicted in Figure 6A. Hall measurements using the van der Pauw geometry are fairly robust, providing that the contacts are placed at the sample corners. Indeed, it has recently been reported that with contacts placed at the corners deviations in the measured carrier concentration occur only in extreme cases of inhomogeneities, such as a center hole, or 100 times greater carrier concentration at the sample edges.[53]

For Hall measurements, a current is passed between probes 1 and 3 (I_{13}) and the Hall voltage, V_H, is measured across probes 2 and 4 (V_{24}) in the presence of a magnetic field that is typically swept between ±3 T. The current is typically swept ±5 nA (although a larger sweep range is used for less resistive samples) at each magnetic field, and the Hall resistance, R_H, is taken as the slope of V_H plotted over the current range. The magnetic field is swept from positive to negative values at least twice with all data points included in the plots. The uncertainty is indicated by the scatter in the data points. A measurement at $B = 0$ T enables determination of the offset voltage (due to asymmetry of the manually applied contacts in the van der Pauw configuration). In the graphs, the offset voltage was not subtracted from the data sets to aid in clarity when comparing the slopes of two similar plots on the same graph. A second permutation is recorded with current passed between contacts 4 and 2, and the Hall voltage is measured between contacts 1 and 3 (V_{13}). All electrical measurements were performed at room temperature.

Acknowledgment. This work was supported partially by NSF-MRSEC Program, by DOE-BES, Grant No. DE-FG02-03ER46028, by the New Zealand Foundation for Research, Science, and Technology (Contract UWIS0501), and by AFOSR. We thank George K. Celler, Soitec, Inc., for providing some of the materials used in these studies. We thank Sangkeun Ha for preliminarily demonstrating to us the low sheet resistance in UTSOI after HF treatment.

REFERENCES AND NOTES

1. Veeraghavan, S.; Fossum, J. G. Short-Channel Effects in SOI MOSFET's. *IEEE Trans. Electron Devices* **1989**, *36*, 522–528.
2. Celler, G. K.; Cristoloveanu, S. Frontiers of Silicon-on-Insulator. *J. Appl. Phys.* **2003**, *93*, 4955–4978.
3. Roberts, M. M.; Klein, L. J.; Savage, D. E.; Slinker, K. A.; Friesen, M.; Celler, G. K.; Eriksson, M. A.; Lagally, M. G. Elastically Relaxed Free-Standing Strained-Silicon Nanomembranes. *Nat. Mater.* **2006**, *5*, 388–393.
4. Scott, S. A.; Lagally, M. G. Elastically Strain-Sharing Nanomembranes: Flexible and Transferable Strained-Silicon and Silicon Germanium Alloys. *J. Phys. D* **2007**, *40*, R75–R92.
5. Menard, E.; Nuzzo, R. G.; Rogers, J. A. Bendable Single Crystal Silicon Thin Film Transistors Formed by Printing on Plastic Substrates. *Appl. Phys. Lett.* **2005**, *86*, 093507.
6. Yuan, H.-C.; Ma, Z. Microwave Thin-Film Transistors Using Si Nanomembranes on Flexible Polymer Substrate. *Appl. Phys. Lett.* **2006**, *89*, 212105.
7. Ko, C. H.; Stoykovich, M. P.; Song, J.; Malyarchuk, V.; Choi, W. M.; Yu, C.-J.; Geddes, J. B.; Xiao, J.; Wang, S.; Huang, Y.; Rogers, J. A. A Hemispherical Electronic Eye Camera Based on Compressible Silicon Optoelectronics. *Nature* **2008**, *454*, 748–753.
8. Mei, Y.; Thurmer, D. J.; Cavallo, F.; Kiravittaya, S.; Schmidt, O. G. Semiconductor Sub-Micro-/Nanochannel Networks by Deterministic Layer Wrinkling. *Adv. Mater.* **2007**, *19*, 2124–2128.
9. Yang, H.; Pang, H.; Qiang, Z.; Ma, Z.; Zhou, W. Surface-Normal Fano Filters Based on Transferred Silicon Nanomembranes on Glass Substrates. *Electron. Lett.* **2008**, *44*, 858–859.
10. Yuan, H.-C.; Shin, J.; Qin, G.; Sun, L.; Bhattacharya, P.; Lagally, M. G.; Celler, G. K.; Ma, Z. Flexible Photodetectors on Plastic Substrates by use of Printing Transferred Single-Crystal Germanium Membranes. *Appl. Phys. Lett.* **2009**, *94*, 013102.
11. Zhang, P. P.; Tevaarwerk, E.; Park, B.-N.; Savage, D. E.; Celler, G. K.; Knezevic, I.; Evans, P. G.; Eriksson, M. A.; Lagally, M. G. Electronic Transport in Nanometre-Scale Silicon-on-Insulator Membranes. *Nature* **2006**, *439*, 703–706.
12. He, T.; He, J.; Lu, M.; Chen, B.; Pang, H.; Reus, W. F.; Nolte, W. M.; Nackashi, D. P.; Franzon, P. D.; Tour, J. M. Controlled Modulation of Conductance in Silicon Devices by Molecular Monolayers. *J. Am. Chem. Soc.* **2006**, *128*, 14537–14541.
13. Boland, J. J. Structure of the H-Saturated Si(100) Surface. *Phys. Rev. Lett.* **1990**, *65*, 3325.
14. Zhang, P. P.; Nordberg, E.; Park, B.-N.; Knezevic, I.; Evans, P. G.; Eriksson, M. A.; Lagally, M. G. Electrical Conductivity in Silicon Nanomembranes. *New J. Phys.* **2006**, *8*, 200.
15. Angermann, H.; Henrion, W.; Rebien, M.; Röseler, A. Wet-Chemical Preparation and Spectroscopic Characterization of Si Interfaces. *Appl. Surf. Sci.* **2004**, *235*, 322–339.
16. Watanabe, D.; En, A.; Nakamura, S.; Suhara, M.; Okumura, T. Anomalously Large Band-Bending for HF-Treated p-Si Surfaces. *Appl. Surf. Sci.* **2003**, *216*, 24–29.
17. Schlaf, R.; Hinogami, R.; Fujitani, M.; Yae, S.; Nakato, Y. Fermi Level Pinning on HF Etched Silicon Surfaces Investigated by Photoelectron Spectroscopy. *J. Vac. Sci. Technol., A* **1999**, *17*, 164–169.
18. Gräf, M.; Grundner, M.; Schulz, R. Reaction of Water wtih Hydrofluoric Acid Treated Silicon (111) and (100) Surfaces. *J. Vac. Sci. Technol., A* **1989**, *7*, 808–813.
19. Huang, L. J.; Lau, W. M. Surface Electrical Properties of HF-Treated Si(100). *J. Vac. Sci. Technol., A* **1992**, *10*, 812–816.
20. Higashi, G. S.; Chabal, Y. J. *Handbook of Semiconductor Wafer Cleaning Technology*; Noyes: Park Ridge, NJ, 1994; p 433.
21. Deal, B. E.; Sklar, M.; Grove, A. S.; Snow, E. H. Characteristics of the Surface-State Charge (Q_{ss}) of Thermally Oxidized Silicon. *J. Electrochem. Soc.* **1967**, *114*, 266–274.
22. Thanh, L. D.; Balk, P. Elimination and Generation of Si-$Si0_2$ Interface Traps by Low Temperature Hydrogen Annealing. *J. Electrochem. Soc.* **1988**, *135*, 1797–1801.
23. Kanungo, P. D.; Zakharov, N.; Bauer, J.; Breitenstein, O.; Werner, P.; Göesele, U. Controlled *In Situ* Boron Doping of Short Silicon Nanowires Grown by Molecular Beam Epitaxy. *Appl. Phys. Lett.* **2008**, *92*, 263107.
24. Cui, Y.; Zhong, Z.; Wang, D.; Wang, W. U.; Lieber, C. M. High Performance Silicon Nanowire Field Effect Transistors. *Nano Lett.* **2003**, *3*, 149–152.
25. Patolsky, F.; Zheng, G.; Lieber, C. M. Fabrication of Silicon Nanowire Devices for Ultrasensitive, Label-Free, Real-Time Detection of Biological and Chemical Species. *Nat. Protoc.* **2006**, *1*, 1711–1724.
26. Angermann, H. Interface State Densities and Surface Charge on Wet-Chemically Prepared Si(100) Surfaces. *Solid State Phenom.* **2005**, *103−104*, 23–26.
27. Dubey, G.; Lopinski, G. P.; Rosei, F. Influence of Physisorbed Water on the Conductivity of Hydrogen Terminated Silicon-on-Insulator Surfaces. *Appl. Phys. Lett.* **2007**, *91*, 232111.
28. Gerardi, G. J.; Poindexter, E. H.; Caplan, P. J. Interface Traps and P_b Centers in Oxidized (100) Silicon Wafers. *Appl. Phys. Lett.* **1986**, *49*, 348–350.
29. Sze, S. M.; Kwok, K. N. *Physics of Semiconductor Devices*, 3rd ed.; John Wiley & Sons: New York, 2007.
30. Yang, J.; de la Garza, L.; Thornton, T. J.; Gust, D. Controlling the Threshold Voltage of a Metal-Oxide-Semiconductor Field Effect Transistor by Molecular Protonation of the Si: SiO_2 Interface. *J. Vac. Sci. Technol., B* **2002**, *20*, 1706–1709.
31. Pavanello, M. A.; Martino, J. A. Extraction of the Oxide Charges at the Silicon Substrate Interface in Silicon-On-Insulator MOSFET's. *Solid-State Electron.* **1999**, *43*, 2039–2046.
32. Pennelli, G.; Piotto, M. Fabrication and Characterization of Silicon Nanowires with Triangular Cross Section. *J. Appl. Phys.* **2006**, *100*, 054507.

33. Yablonovitch, E.; Allara, D. L.; Chang, C. C.; Gmitter, T.; Bright, T. T. Unusually Low Surface-Recombination Velocity on Silicon and Germanium Surfaces. *Phys. Rev. Lett.* **1986**, *57*, 249–252.
34. Thornton, J. M. C.; Williams, R. H. A Photoemission-Study of Passivated Silicon Surfaces Produced by Etching in Solutions of HF. *Semicond. Sci. Technol.* **1989**, *4*, 847–851.
35. Huang, L. J.; Lau, W. M. Effects of HF Cleaning and Subseqent Heating on the Electrical Properties of Silicon (100) Surfaces. *Appl. Phys. Lett.* **1992**, *60*, 1108–1110.
36. Boland, J. J. Scanning-Tunneling-Microscopy of the Interaction of Hydrogen with Silicon Surfaces. *Adv. Phys.* **1993**, *42*, 129–171.
37. Takahagi, T.; Ishitani, A.; Kuroda, H.; Nagasawa, Y. Fluorine-Containing Species on the Hydrofluoric Acid Etched Silicon Single-Crystal Surface. *J. Appl. Phys.* **1991**, *69*, 803–807.
38. Grundner, M.; Schulz, R. The Surface State of Si(100) and (111) Wafers after Treatment with Hydrofluoric Acid. *AIP Conf. Proc.* **1987**, *167*, 329–337.
39. Awakuni, Y.; Calderwood, J. H. Water Vapour Adsorption and Surface Conductivity in Solids. *J. Phys. D* **1972**, *5*, 1038–1045.
40. Liu, D.; Wang, Q.; Paravi, H.; Drobny, V.; Moquin, J. Detecting Impurities in the Ultra Thin Silicon Oxide Layer by Hg-Schottky Capacitance−Voltage (CV) Method. *Mater. Res. Soc. Symp. Proc.* **2001**, *670*, K7.7.1K7.7.6.
41. Sun, J.; Chen, J.; Wang, X.; Wang, J.; Liu, W.; Zhu, J.; Yang, H. Stress Evolution Influenced by Oxide Charges on GaN Metal-Organic Chemical Vapor Deposition on Silicon-on-Insulator Substrate. *Appl. Phys. A: Mater. Sci. Process.* **2007**, *89*, 177–181.
42. Hamaide, G.; Allibert, F.; Hovel, H.; Cristoloveanu, S. Impact of Free-Surface Passivation on Silicon on Insulator Buried Interface Properties by Pseudotransistor Characterization. *J. Appl. Phys.* **2007**, *101*, 114513.
43. Seo, K.; Sharma, S.; Yasseri, A. A.; Stewart, D. R.; Kamins, T. I. Surface Charge Density of Unpassivated and Passivated Metal-Catalyzed Silicon Nanowires. *Electrochem. Solid-State Lett.* **2006**, *9*, G69–G72.
44. Schmidt, V.; Senz, S.; Gösele, U. Influence of the Si/SiO_2 Interface on the Charge Carrier Density of Si Nanowires. *Appl. Phys. A: Mater. Sci. Process.* **2007**, *86*, 187–191.
45. Patolsky, F.; Zheng, G.; Hayden, O.; Lakadamyali, M.; Zhuang, X.; Lieber, C. M. Electrical Detection of Single Viruses. *Proc. Natl. Acad. Sci. U.S.A.* **2004**, *101*, 14017–14022.
46. Zheng, G.; Patolsky, F.; Cui, Y.; Wang, W. U.; Lieber, C. M. Multiplexed Electrical Detection of Cancer Markers with Nanowire Sensor Arrays. *Nat. Biotechnol.* **2005**, *23*, 1294–1301.
47. Yang, J.; Thornton, T. J.; Kozicki, M.; de la Garza, L.; Gust, D. Molecular Control of the Threshold Voltage of an NMOS Inversion Layer. *Microelectron. Eng.* **2002**, *63*, 135–139.
48. Nikolaides, M. G.; Rauschenbach, S.; Luber, S.; Buchholz, K.; Tornow, M.; Abstreiter, G.; Bausch, A. R. Silicon-on-Insulator Based Thin-Film Resistor for Chemical and Biological Sensor Applications. *ChemPhysChem* **2003**, *4*, 1104–1106.
49. Lasseter, T. L.; Clare, B. H.; Abbott, N. L.; Hamers, R. J. Covalently Modified Silicon and Diamond Surfaces: Resistance to Nonspecific Protein Adsorption and Optimization for Biosensing. *J. Am. Chem. Soc.* **2004**, *126*, 10220–10221.
50. Lin, Z.; Strother, T.; Cai, W.; Cao, X. P.; Smith, L. M.; Hamers, R. J. DNA Attachment and Hybridization at the Silicon (100) Surface. *Langmuir* **2002**, *18*, 788–796.
51. Euaruksakul, C.; Li, Z. W.; Zheng, F.; Himpsel, F. J.; Ritz, C. S.; Tanto, B.; Savage, D. E.; Liu, X. S.; Lagally, M. G. Influence of Strain on the Conduction Band Structure of Strained Silicon Nanomembranes. *Phys. Rev. Lett.* **2008**, *101*, 147403.
52. van der Pauw, L. J. A Method of Measuring Specific Resistivity and Hall Effect of Discs of Arbitrary Shape. *Philips Res. Repts.* **1958**, *13*, 1–9.
53. Bierwagen, O.; Ive, T.; Van de Walle, C. G.; Speck, J. S. Causes of Incorrect Carrier-Type Identification in van der Pauw−Hall Measurements. *Appl. Phys. Lett.* **2008**, *93*, 242108.